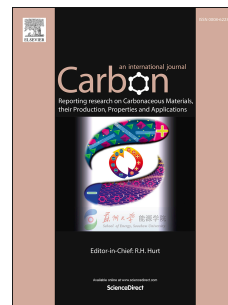


Journal Pre-proof

Facile and environmentally friendly synthesis of ultramicroporous carbon spheres: a significant improvement in CVD method

Saeed Khodabakhshi, Sajad Kiani, Yubiao Niu, Alvin Orbaek White, Wafa Suwaileh, Richard E. Palmer, Andrew R. Barron, Enrico Andreoli



PII: S0008-6223(20)30822-8

DOI: <https://doi.org/10.1016/j.carbon.2020.08.056>

Reference: CARBON 15608

To appear in: *Carbon*

Received Date: 5 July 2020

Revised Date: 18 August 2020

Accepted Date: 23 August 2020

Please cite this article as: S. Khodabakhshi, S. Kiani, Y. Niu, A.O. White, W. Suwaileh, R.E. Palmer, A.R. Barron, E. Andreoli, Facile and environmentally friendly synthesis of ultramicroporous carbon spheres: a significant improvement in CVD method, *Carbon*, <https://doi.org/10.1016/j.carbon.2020.08.056>.

This is a PDF file of an article that has undergone enhancements after acceptance, such as the addition of a cover page and metadata, and formatting for readability, but it is not yet the definitive version of record. This version will undergo additional copyediting, typesetting and review before it is published in its final form, but we are providing this version to give early visibility of the article. Please note that, during the production process, errors may be discovered which could affect the content, and all legal disclaimers that apply to the journal pertain.

© 2020 Elsevier Ltd. All rights reserved.

AUTHORSHIP STATEMENT

Manuscript title:

Facile and environmentally friendly synthesis of ultramicroporous carbon spheres: a significant improvement in CVD method

All persons who meet authorship criteria are listed as authors, and all authors certify that they have participated sufficiently in the work to take public responsibility for the content, including participation in the concept, design, analysis, writing, or revision of the manuscript. Furthermore, each author certifies that this material or similar material has not been and will not be submitted to or published in any other publication before its appearance in CARBON.

Authorship contributions

Category 1

Conception and design of study: Saeed Khodabakhshi, Enrico Andreoli

acquisition of data: Saeed Khodabakhshi, Sajad Kiani, Yubiao Niu, Alvin Orbaek White, Wafa Suwaileh.

Analysis and/or interpretation of data: Saeed Khodabakhshi, Sajad Kiani, Yubiao Niu, Alvin Orbaek White, Wafa Suwaileh, Richard E. Palmer, Andrew R. Barron, Enrico Andreoli.

Category 2

Drafting the manuscript: Saeed Khodabakhshi, Enrico Andreoli, Richard E. Palmer, Andrew R. Barron.

Revising the manuscript critically for important intellectual content: Andrew R. Barron.

Category 3

Approval of the version of the manuscript to be published (the names of all authors must be listed): Saeed Khodabakhshi, Sajad Kiani, Yubiao Niu, Alvin Orbaek White, Wafa Suwaileh, Richard E. Palmer, Andrew R. Barron, Enrico Andreoli.

Facile and environmentally friendly synthesis of ultramicroporous carbon spheres: a significant improvement in CVD method

Saeed Khodabakhshi,^{*a} Sajad Kiani,^a Yubiao Niu,^b Alvin Orbaek White,^a Wafa Suwaileh,^b

Richard E. Palmer,^b Andrew R. Barron,^{a,c,d} Enrico Andreoli^{*a}

^aEnergy Safety Research Institute, Swansea University, Bay Campus, Swansea SA1 8EN, U.K.

^bCollege of Engineering, Swansea University, Bay Campus, Swansea, SA1 8EN, U.K.

^cDepartment of Chemistry and Department of Materials Science and Nanoengineering, Rice University, Houston, Texas 77005, U.S.A.

^dFaculty of Engineering, Universiti Teknologi Brunei, Jalan Tungku Link, Gadong, BE1410, Brunei Darussalam

E-mail: saeid.khodabakhshi@swansea.ac.uk; e.andreoli@swansea.ac.uk

Facile and environmentally friendly synthesis of ultramicroporous carbon spheres: a significant improvement in CVD method

Saeed Khodabakhshi,^{*a} Sajad Kiani,^a Yubiao Niu,^b Alvin Orbaek White,^a Wafa Suwaileh,^b

Richard E. Palmer,^b Andrew R. Barron,^{a,c,d} Enrico Andreoli^{*a}

^aEnergy Safety Research Institute, Swansea University, Bay Campus, Swansea SA1 8EN, U.K.

^bCollege of Engineering, Swansea University, Bay Campus, Swansea, SA1 8EN, U.K.

^cDepartment of Chemistry and Department of Materials Science and Nanoengineering, Rice University, Houston, Texas 77005, U.S.A.

^dFaculty of Engineering, Universiti Teknologi Brunei, Jalan Tungku Link, Gadong, BE1410, Brunei Darussalam

E-mail: saeid.khodabakhshi@swansea.ac.uk; e.andreoli@swansea.ac.uk

Abstract

A new and environmentally friendly non-caustic route to synthesize ultramicroporous carbon spheres (CS) via a simple one-step non-catalytic and activation-free chemical vapor deposition (CVD) method is described. The CVD method was applied at different temperatures, 600-900 °C; 800 °C was identified as the optimum for CS formation using a safe solid feedstock. The proposed method is suitable for large-scale adoption since high pyrolysis temperatures are already used in multi-million-ton industries such as that of carbon black production. Specific surface area and total pore volume were influenced by the deposition temperature, leading to an appreciable change in overall capture capacity. The ultramicropores allow the effective interaction of the sorbent with CO₂, resulting in high carbon capture capacity at both atmospheric and lower pressures. At atmospheric pressure, the highest CO₂ adsorption capacities were ca. 4.0 mmol.g⁻¹ and 2.9 mmol.g⁻¹ at 0 °C and 25 °C, respectively, for the best CS. At lower pressure, 0.15 bar, the CO₂ adsorption capacities were 2.0 mmol.g⁻¹ and 1.1 mmol.g⁻¹, again at 0 °C and 25 °C. The CS showed good sorption/desorption cyclability, ease of regeneration, favorable selectivity over N₂ of 30:1 at 25 °C, and rapid kinetics.

KEYWORD: Carbon spheres, Ultramicropores, CVD, Green, CO₂ capture.

1. Introduction

Carbon spheres (CS) ranging in size from nanometers to micrometers have received considerable attention over the past decade due to their outstanding role in some applications such as energy storage and conversion, catalysis, gas adsorption and storage, drug and enzyme delivery, and water treatment [1-3]. So far, several pathways have been developed for the synthesis of CS,[4] including nanocasting with silica spheres as hard templates,[5] hydrothermal carbonization of carbohydrates [6], chemical vapour deposition (CVD) [7, 8], modified Stöber synthesis [9], soft-templating methods [10-12], plasma [13], Friedel–Craft reaction-induced polyaromatic precursors [14], spray pyrolysis [15], etc. The reports are mainly based on expensive and impractical methods involving multi-step processes and difficult purification such as template removal [16]. Furthermore, some of these methods lead to non-porous spheres with low surface area or nonuniformly shaped particles limiting their application. Biomass-derived compounds have also been used to prepare CS. However, they requires an initial hydrothermal process followed by activation under CO₂ and carbonization [17]. Regardless of carbon particle morphology, almost all other porous carbon derived from biomass require additional physical and chemical activations while not all can deliver ultramicroporosity [18]. However, to the best of our knowledge, there is no report on the synthesis of CS using biomass feedstock via CVD.

Over the past decade, CVD has been increasingly applied for the large scale preparation of nanocarbons such as CNTs [19, 20], graphene [21, 22], carbon spheres [7], etc. However, at present, all CVD methods for CS production require toxic or flammable liquid/gas feedstocks. Also, CVD methods rely on the use of costly catalysts for sphere growth, and corrosive work-up procedures to remove the catalyst from the final product. Altogether, ultramicroporous carbon spheres are not facile to synthesis via conventional methods [4].

Public concern about global warming, climate change, and man-made green-house gas emissions, is ever increasing. Among greenhouse gases, CO₂ makes contribution to the current global climate change [23, 24]. The steady increase in atmospheric CO₂ concentration is linked to the burning of fossil fuels to fulfil the world's energy demands, however, the need for fossil fuels will continue until they are entirely replaced with clean and renewable sources. One of the potentially effective measures against climate change is the use of low-cost, practical technologies to capture and sequester CO₂ emissions from source points.[25] Amongst the established materials for post-combustion CO₂ capture, aqueous amine solutions are the most used and cheap sorbents, but chemisorption remains

energy-intensive (since the energy penalty of amine regeneration is high) and corrosive. Although the energy required to recycle the amine functionality may be lowered by incorporation of carbon nanomaterials [26, 27], the reactions of amines with acidic components of combustion gas or amine oxidative degradation, add to environmental concerns [25]. As a result, physisorption with porous materials such as activated carbon (AC) [28, 29], zeolites [30], supported amines [31, 32], metal oxides [33], and metal-organic frameworks (MOFs) [34], have become increasingly popular and are being rapidly developed as suitable alternatives for CO₂ capture. Each type of material may come with drawbacks, e.g., most MOFs or zeolites, despite having high CO₂ uptake, suffer from a performance decay in humid flue gases [35]. Among all promising capture materials, porous carbons have received significant attention as a result of their low cost and wide availability, hydrophobicity, high stability and surface area, ease of preparation, good recyclability, and moderate heat of adsorption [28].

In this work, a low-cost and catalyst-free CVD method is described for the production of uniform oxygen-doped CS using pyromellitic acid as both carbon and oxygen source. The CO₂ capture efficiency of the spheres was studied at different pressures and temperatures. Due to the presence of ultramicropores, the non-activated CS achieved excitedly good CO₂ adsorption capacity and selectivity (over N₂) comparable or even better than activated carbon spheres previously reported in the literature [16, 36-42].

2. Experimental

2.1. General method

CO₂ adsorption set-up (Fig. S1) are explained in detail in the Supplementary Information. Scanning transmission electron microscopy (STEM) and high-resolution transmission electron microscopy (HRTEM) images of the spheres were performed using a FEI Talos F200X Transmission Electron Microscope. The selected area electron diffraction (SAED) pattern was taken from TEM mode under 200 keV electron beam without sample tilt. Energy dispersive X-ray spectroscopy (EDS) was conducted on a carbon grid. Scanning electron microscopy (SEM) images of the spheres were obtained with a JEOL 7800F FEG SEM (JEOL, Akishima, Tokyo, Japan).

The Raman data of the carbon spheres were recorded at room temperature using a Renishaw inVia Raman Microscope (Renishaw plc, Miskin, Pontyclun, UK) with excitation wavelength of 457, 514, and 633 nm. The elemental analyzer (vario EL cubewas, Germany) was used to determine the amount of carbon, hydrogen and oxygen.

The samples were characterized using a Thermo Scientific Nicolet iS10 FT-IR Spectrometer. Thermogravimetric analysis (TGA) was carried out using 10-mg sample placed in an alumina pan with a TA Instruments SDT Q600 at a heating rate of 5 °C.min⁻¹ from room temperature to 900 °C in air. N₂ adsorption/desorption isotherms were obtained using a Quadrosorb SI (Quantachrome Instruments, Boynton Beach, FL, USA). Specific surface areas were calculated based on the Brunauer–Emmett–Teller (BET) method, and pore size distribution was determined using the non-localized density functional theory (NL-DFT) method. X-ray photoelectron spectroscopy (XPS) was performed using a Kratos Axis Supra (Kratos Analytical, Japan) utilizing a monochromatic Al-K_α X-ray source (K_α 1486.58 eV), 15 mA emission current, magnetic hybrid lens, and slot aperture. Region scans were performed using a pass energy of 40 eV and step size of 0.1 eV. Peak fitting of the narrow region spectra was performed using a Shirley type background, and the synthetic peaks were of a mixed Gaussian-Lorentzian type. Carbon sp² was used for charge reference assumed to have a binding energy of 284 eV. The thermal synthesis reactions were carried out in a two-zone furnace (SSP-354 Reactor, Nanotech Innovations, 132 Artino St., Oberlin, OH, USA) using a quartz tube (38mm OD, 34mm ID, 762mm L) and an alumina-ceramic combustion boat (70mm L, 15mm OD, 12mm ID). Powder X-ray diffraction (XRD) patterns were collected in the 1-60° 2θ range with a Bruker D8 Avance diffractometer using Cu K_{α1} radiation (λ = 1.54060 Å). Static contact angles of carbon sphere coatings were measured using a DSA25 Expert Drop Shape Analyzer equipped with an automated camera and ADVANCE software (KRÜSS GmbH).

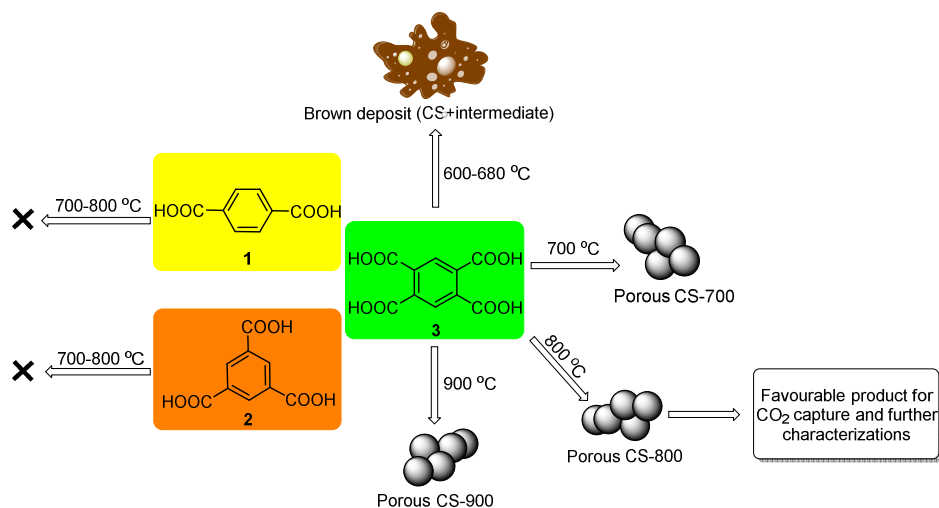
2.2. Synthesis of CS by CVD

Pyromellitic acid (96%) was purchased from Sigma-Aldrich and used without further purification. A two-zone tubular furnace was used for the pyrolysis under argon (200 mL.min⁻¹) at atmospheric pressure, with the temperature of each zone controlled independently, and all materials flowing from the first zone (Zone 1) to the second one (Zone 2). In a typical procedure, 1 g of acid precursors (e.g. pyromellitic acid) was placed in a alumina-ceramic boat and inserted into the Zone 1. Under argon (200 mL.min⁻¹), the temperature of Zone 2 was set then raised to a value between 600 and 900 °C at an average rate of 60 °C.min⁻¹, as detailed later in the manuscript. When the desired temperature of Zone 2 was reached, the temperature of Zone 1 was increased from room temperature to 450 °C at an average rate of 60 °C.min⁻¹ and held at that temperature for 30 min. All

pyrolyses were performed with Zone 1 at 450 °C for pyromellitic acid and 450-700 °C for trimesic acid. Finally, the furnace was cooled down to room temperature still under argon, and the CS (0.17 g) were collected from the inside wall of the quartz tube in Zone 2 and used without any further processing. It is worth mentioning that the process for production of 1g of CS-800 (as desired product) requires approximately 52 min. Fig. S2a and S2b represent the CVD set-up and boat containing precursor, respectively.

3. Results and discussion

Following our studies on the manipulation of CS [43] for CO₂ capture [44-46], we turned our attention to green methods focusing on CVD of different benzene carboxylic acids (BCAs) as feedstock to produce porous carbon spheres. Scheme 1 presents a thermal treatment method applied to three precursors, terephthalic acid **1**, trimesic acid **2**, and pyromellitic acid **3**, in the attempt to produce CS. The precursors, starting points of the CVD, are highlighted in green, yellow and orange. When terephthalic acid **1** was used, it left no carbon residue in either Zone 1 or Zone 2 of the furnace at any of the tested temperatures. Instead, a very small residue of carbonaceous material was found left in the ceramic boat upon heating trimesic acid **2** to 450 °C in Zone 1. However, after raising the temperature of Zone 1 to 700 °C, no pyrolyzed carbon residue of trimesic acid **2** was found in the boat. It is relevant to note that trimesic acid has a predicted boiling point of ca. 560 °C, which is higher than that of terephthalic acid of ca. 230 °C in a closed tube. Terephthalic acid sublimates at ca. 270 °C under atmospheric pressure. Therefore, the thermal treatment of **1** leads to sublimation since no degradation products have been observed at temperatures below 445 °C [47], whereas **2** leaves a trace residue upon pyrolysis at 450 °C, but not at 700 °C.



Scheme 1. Precursors and temperatures evaluated to produce CS. Precursors: terephthalic acid (yellow), trimesic acid (orange), and pyromellitic acid (green). CS were formed only from pyromellitic acid, no products were collected when terephthalic acid or trimesic acid was used. All temperatures refer to Zone 2, where CS formed. The temperature of Zone 1 was fixed to 450 °C for all pyrolyses.

Remarkably, an entirely different behavior was observed in the case of pyromellitic acid **3**. The thermal treatment of **3** left no trace of residual material in the ceramic boat placed in Zone 1 (450 °C) while a series of carbonized materials were found in Zone 2 set at different temperatures ranging from 600 °C to 900 °C. More specifically, for temperatures between 600 °C and 680 °C a brown deposit was collected after Zone 2, the deposit containing some CS. Upon raising the temperature of Zone 2 above 700 °C, all pyromellitic acid **3** was converted to an inner wall black deposit entirely made of CS, *vide infra*. Upon a closer examination of the brown deposits formed at temperatures below 700 °C, it was established that these were mixtures of CS and an additional component that was determined to be an intermediate of chemical vapor deposition of the CS. After separation and characterization, it was established that intermediate was pyromellitic dianhydride which is known to be formed upon thermal dehydration of pyromellitic acid [48, 49]. It is assumed that the thermal decomposition of pyromellitic dianhydride in Zone 2 is the key process upon which carbon sphere nuclei are formed, as discussed in detail later. In particular, the carbon sphere product obtained at 800 °C (CS-800) showed the best CO₂ capture performance, also discussed later.

3.1. Materials characterization

Fig. 1a shows the FT-IR spectra of precursor (pyromellitic acid), intermediate (found in the brown deposit, Scheme 1), and final product (CS-800, carbon spheres in Fig. 2). Two key differences are observed between the spectra of precursor (red spectrum) and intermediate (blue spectrum). First, the C=O stretching band for pyromellitic acid at 1700 cm⁻¹, typical of carboxylic acid, is found at 1800 cm⁻¹ in the spectrum of the intermediate, which is characteristic of anhydride. Second, the broad OH stretching bands at 3000 cm⁻¹ in the spectrum of the precursor are not present in that of the intermediate, additional evidence of the conversion of the carboxylic group to anhydride. These results confirm the thermal conversion pyromellitic acid to pyromellitic anhydride[48, 49] which appears to

be a key intermediate of carbon spheres formation. The infrared spectrum of CS-800 present characteristic features corresponding to the stretching vibrations of C=O (1450–1700 cm^{-1}). Fig. 1b shows the Raman spectra of CS-800 recorded at two different wavelengths 457 nm and 514 nm, both spectra clearly show peaks arising from sp^2 and sp^3 carbons at $\sim 1350 \text{ cm}^{-1}$ and $\sim 1580 \text{ cm}^{-1}$, respectively. In both cases the intensity of G band was higher than D band representing more sp^2 carbon in the CS structure. I_D/I_G were also calculated as 0.6 and 0.8 for 457 and 514 nm, respectively. In addition, we note the presence of several broad peaks in the region of 2500–2800 cm^{-1} which is known as fluorescent background as a result of functional groups [50, 51]. In addition, they can be likely to be both the overtones of the D and G peak and from stochastic connections between CS. As such, the Raman spectra suggest both an amorphous nature for the as-synthesized CS with a covalent random network including both sp^3 and sp^2 hybridization while the sp^2 G-peak is dominant. Raman Spectra for CS-700 and CS-900 can be also seen in the Supplementary Information (Fig. S3).

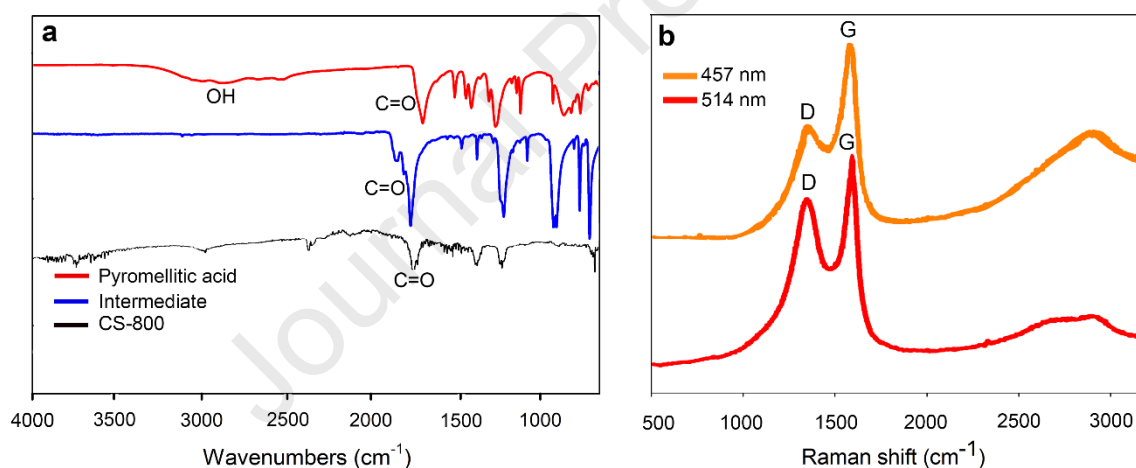


Fig. 1. FT-IR spectra of pyromellitic acid precursor (red), intermediate of CS formation (blue), and CS (black) (a), and Raman spectra for CS-800 at different wavelength (b).

As can be seen in Fig. 2a, the SEM image for CS-800 shows a large agglomerate of aggregated material, component spheres are visible in Fig. S4. In addition, TEM and scanning transmission electron microscopy (STEM) revealed a spherical morphology with an average diameter of 200 nm. However, the images did not show evidence of porosity in the carbon spheres due to the beam-sensitivity of carbon-based materials [52]. CS-700 and CS-900 have similar morphology to CS-800, as evident in the SEM images of Fig. S4, which also shows the stem-like morphology for the residue of carbonaceous materials in

Zone 1 confirming the spheres are only formed by CVD process. The energy dispersive X-Ray spectroscopy (EDS) mapping analysis of the CS is shown in Fig. 3 with a carbon content of 96.3 at.% and an oxygen content of 3.6 at.%. These results are in close agreement with those recorded from the elemental analysis, with C and O contents of 92.6 at.% and 5.6 at.%, respectively.

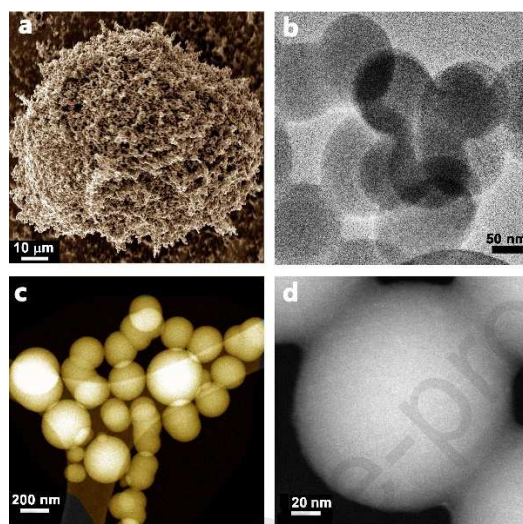


Fig. 2. SEM image (a), TEM image (b), STEM images (c and d) of CS-800 obtained by CVD method. SEM shows agglomerated spheres while single spheres in the range of 100-300 nm can be seen from STEM and TEM.

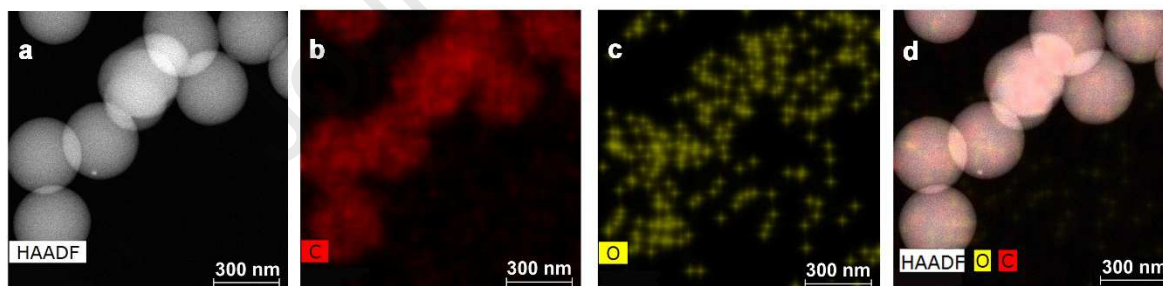


Fig. 3. High-angle annular dark-field (HAADF)-STEM image (a), carbon and oxygen elemental mappings (b and c, respectively) of CS-800. The STEM image and elemental mappings were superimposed to give the image (d) showing the even distribution of carbon and oxygen in the spheres. (A color version of this Fig. can be viewed online).

The carbon spheres were characterized with SAED (Fig. S5a), showing no clearly defined diffraction pattern and crystalline structure for CS-800. In addition, the X-ray diffraction (XRD) spectrum also confirmed the substantially amorphous nature of CS-800

(Fig. S5b) with only two very broad peaks because of the a axis of the graphite structure, at $2\theta = 24^\circ$ and 42° attributed to the reflections of (002) and (101) planes, respectively [53]. It appears that the carbon spheres are mostly amorphous with both sp^2 and sp^3 carbons coexisting in domains lacking of grain boundaries [54].

The surface composition of CS-800 was analyzed using XPS. The survey spectrum (Fig. 4a) confirms the presence of only two elements, carbon and oxygen in atomic concentrations of 94.7 at.% and 5.3 at.%, respectively. The oxygen content on the surface is higher than that measured for the bulk, where 3.5 at.% (5.6 wt.%) oxygen was determined from elemental analysis, as previously mentioned. This corresponds to a greater level of oxygen doping on the external surface of the CS. The C1s narrow region spectrum was deconvoluted in four peaks (Fig. 4b). A main contribution to the intensity of the signal is due to sp^2 carbon (green peak) at binding energy 284.0 eV, while the sp^3 carbon component is found at 285.3 eV (blue peak) [55]. There are also peaks related to oxidized carbon, C-O at 286.6 eV (light blue peak), and C=O at 288.1 eV (yellow peak) [56]. Graphitic $\pi-\pi^*$ shake-up satellites were fitted with a broad peak centered at 290.1 eV [56]. These results highlight the presence of partially oxidized structures, and the O1s narrow region spectrum supports these observations (Fig. 4c). The oxygen signal was deconvoluted into two peaks, an O=C peak at binding energy 531.7 eV (fuchsia peak) and a O-C peak at 533.2 eV (red peak). The corresponding O=C/O-C oxygen atomic ratio is 1.8 [56].

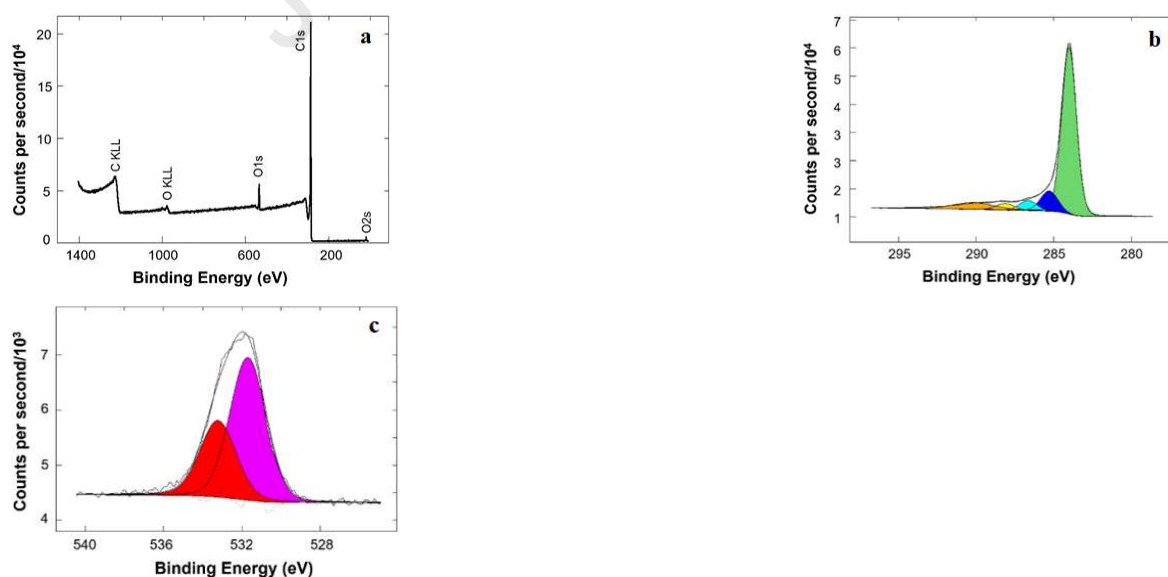


Fig. 4. XPS characterization of CS-800. Survey spectrum showing that carbon and oxygen are the only elements detected on the surface of the sample (a). C1s narrow

region spectrum of sample CS-800; peak fitting is color coded C=C sp^2 (green), C-C/H sp^3 (blue), C-O (light blue), C=O (yellow), and $\pi-\pi^*$ shake-up satellite (orange) (b). O1s narrow region spectrum of sample CS-800; peak fitting is color coded O=C (purple), and O-C (red) (c).

CS form at temperatures in the range of 700-900 °C from precursor 3, and their textural properties such as surface area and pore volume are slightly different. To investigate the effect of carbonization temperature on the CO₂ capture capacity, surface areas and pores size distributions of CS were determined from N₂ and CO₂ adsorption measurements (Fig. S6a,b). BET surface areas were estimated using N₂ at 77 K, while pore size distributions were calculated using NL-DFT [57] with data collected using CO₂ at 273 K. Fig. S6a demonstrates that all synthesized CS have type-I curves (IUPAC classification) [58]. A high abundance of micropores in CS is confirmed by a sharp rise in N₂ adsorption at a low relative pressure ($P/P_0 < 0.01$) [59]. Fig. 5 presents the pore distributions for all as-synthesized CS in the range below 1 nm (pore diameter = 2 times the half pore width) confirming the presence of narrow micropores which are mainly responsible for CO₂ capture at low pressures. As can be seen from Table 1, the micropore volume and surface area change by change in carbonization temperature. Based on our observation, the surface area for CS-900 and CS-700 are similar, while CS-800 shows the highest surface area. Besides, the micropore volume for each sample measured by CO₂ shows a significant difference between CS-700 and C-900 while CS-900 and CS-800 are closer. In other words, CS obtained at 800 °C contains more total pore volume and micropore volume (calculated by both N₂ and CO₂) than those obtained at 700 °C and 900 °C which can confirm the key effect of Zone 2 temperature on the textural properties of these CVD products. Table 1 also lists C, O, H content of CS measured by elemental analysis as determined by an average of three runs.

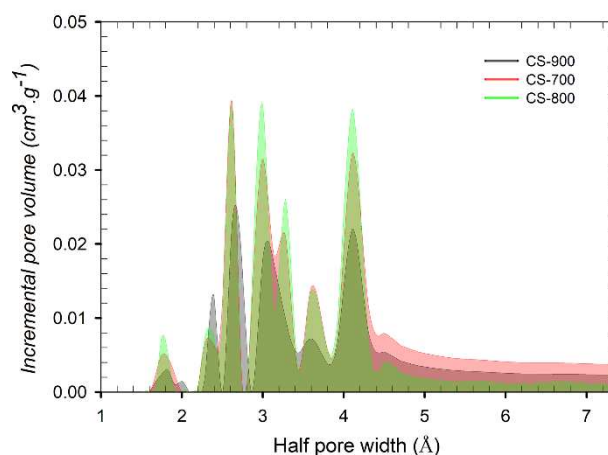


Fig. 5. Pore size distributions of CS samples measured using CO₂ at 273 K and calculated by NL-DFT method. All pore diameters are less than 0.9 nm. Darker areas are the result of overlapping distributions.

Table 1. Textural parameters obtained from N₂ (77 K) and CO₂ (273 K) adsorption data and elemental analysis for synthesized CS.

Sample	S _{BET} (m ² .g ⁻¹) ^a	V _{total} (cm ³ .g ⁻¹) ^b	V _{micro} (cm ³ .g ⁻¹) ^b	V _{total} (cm ³ .g ⁻¹) ^a	V _{micro} (cm ³ .g ⁻¹) ^a	V _{meso} (cm ³ .g ⁻¹) ^a	Elemental content (wt.%)		
							C	H	O
CS-900	635	0.156	0.129	0.275	0.247	0.022	94.8	1.9	3.3
CS-800	804	0.192	0.128	0.340	0.294	0.038	92.6	1.8	5.6
CS-700	639	0.168	0.082	0.277	0.251	0.028	85.8	2.4	11.8

^aObtained from N₂ adsorption at 77 K. ^bObtained from CO₂ adsorption at 273 K.

Thermogravimetric analysis (TGA) under air flow was used to check the thermal stability of CS between 23 °C and 900 °C. The TG profile for the synthesized CS shows a similar oxidation behavior to those previously reported in the literature with an initial weight decrease below 200 °C attributed to loss of water and volatile components adsorbed on the surface. Subsequently, another mass loss is observed between 200 °C and 400 °C which likely corresponds to surface functional group decomposition. A dominant weight drop is eventually seen between 450-580 °C due to the thermal oxidation of the spheres (Fig. S7). The combustion of CS-800 left a trace of incombustible material (<1 w%), which was associated to resulting ash.

The wettability of a uniform coating of CS-800 sprayed on a glass slide was also evaluated via water contact angle measurements (Fig. S8 and S9). A contact angle of 161.5° was measured showing the superhydrophobic nature of the CS-800 coating. The surface roughness of the coating and morphology of the carbon spheres would also contribute the hydrophobicity. The high hydrophobicity along with the presence of narrow micropores should make CS-800 an ideal adsorbent for CO₂ capture in humid conditions which is discussed later.

3.2. Comparison of existing methods for synthesis of CS

It is important to note that CVD methods to date failed to produce microporous carbon spheres even when expensive catalysts were used, as we listed in Table 2. It should be also noted that high temperature plays a critical role in CVD, consequently, the process requires important safety measures when hazardous flammable feedstocks are employed (e.g., acetylene and ethylene). Therefore, using a solid feedstock such as mellitic acid benefits from easier handling and lower risks.

The porosity of the CS listed in Table 2 is less if not developed at all compared to the microporosity of our CS, the merits of our pathway is then evident among other CVD methods to generate porous carbon spheres. Compared to the catalyst-free method listed in Table 2 which gives non-porous CS, we can assume that our non-catalytic strategy leads to microporous CS due to the presence of COOH groups while it does not exist in the structure of toluene and styrene. In other words, releasing CO₂ during decomposition can develop microporosity similar to the strategy used for activated carbon production using CO₂ as activator [60]. As can be seen, the CVD method mainly feeds on hydrocarbon gases and liquids such as acetylene and benzene and demands a metal catalyst or silica-based template, while we used a solid feedstock without catalyst. This is a significant improvement since both catalyst price and catalyst removal as well as hazards of highly flammable and toxic gas or liquid feedstocks are drawbacks of these approaches. Furthermore, our catalyst-free strategy makes carbon nanospheres that are smaller than those of the other methods, ca. 200 nm diameter, also at lower or comparable pyrolysis temperature [5, 8, 61-65]. Although the main factor affecting the sphere size in our method is still unclear, we observed that the temperature slightly affects the size of spheres while it has significant influence on the sphere uniformity. Accordingly, the more uniform CS was formed at lower temperatures of 700 °C and 800 °C. The most uniform spheres were observed from SEM for CSs made at 700 °C, while it has less surface area and micropore volume (Fig. S4).

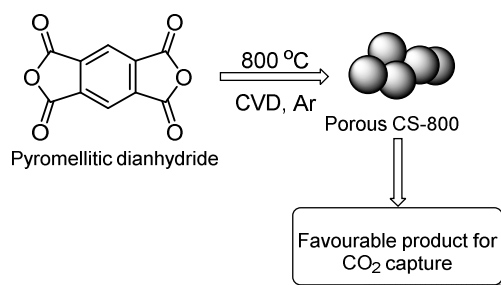
Table 2. Comparison of present CVD method with previously reported CVD methods in the literature for synthesis of CS.

Carbon feedstock	Catalyst	Deposition Temperature (°C)	Porosity type	Sphere size average (nm)
------------------	----------	-----------------------------	---------------	--------------------------

Ethylene	NiFe-LDHs [61]	900	Non-porous	740
Acetylene	Fe-KIT-6 [8]	800	Meso	750
Ethylene	Kaolin supported transition metal [62]	750-900	Not measured	400 and 2000
Ethylene	Mesoporous silica template [63]	800	Meso	260
Ethylene	Mesoporous silica template [5]	800	Meso	400
Polypropylene	Mesoporous silica template [64]	900	Non-porous	1000
Styrene, toluene, benzene, hexane, cyclohexane and ethene	Free [65]	900-1200	Non-porous	300-700
Pyromellitic acid	Free ^a	700-900	Microporous	200

^aThis work.

The exact mechanism of chemical vapor deposition for catalyst-free CS formation is still not fully understood since the collapse and recombination of the chemical structures during carbonization is difficult to rationalize. It can be assumed that the pathway of formation of spheres might be similar to that reported for soot spherical particles [66, 67]. However, it is worth to note that during our experiment, we could find out that dehydration of pyromellitic acid occurs before its decomposition. To confirm the formation of pyromellitic dianhydride from the dehydration of pyromellitic acid in Zone 1, a separate experiment was conducted with Zone 1 at 450 °C and Zone 2 at room temperature. A white powder deposit was found on the inner wall of the tube at the non-heated end of the furnace. Upon comparison of the FT-IR spectra of white powder and commercial pyromellitic dianhydride, there was no appreciable difference between the two confirming that the white powder was pyromellitic dianhydride (Fig. S10). This finding directed us towards using either commercial pyromellitic dianhydride or the one separated as intermediate during the process in place of pyromellitic acid which resulted in the same product (Scheme 2).



Scheme 2. Production of CS by CVD method from pyromellitic dianhydride under argon. Temperature refers to Zone 2, where CS are deposited. The temperature of Zone 1 was 450 °C.

However, pyromellitic dianhydride is classified as hazardous material according to EC Regulation No 1272/2008. Therefore, using pyromellitic acid as a non-toxic precursor material meets Green Chemistry principles [68].

3.3. Carbon dioxide capture

Using a volumetric gas sorption apparatus, the CO₂ capture performance of as prepared CS was assessed in the pressure range from vacuum to 10 bar at four different temperatures, 0, 25, 35, and 45 °C. Fig. 6 presents data collected at 0 and 25 °C. At 25 °C, CS-700 achieved the highest capture capacity at 10 bar, 5.4 mmol.g⁻¹ (Fig. 6a), however at lower pressure CS-800 performed better than CS-700 and CS-900, with capture capacities of 1.1 mmol.g⁻¹ and 2.85 mmol.g⁻¹ at 0.15 bar and 1 bar, respectively (Fig. 6b). The porosity of the CS plays a major role in achieving this performance. In particular, pores with diameters smaller than 10 Å are suitable for CO₂ adsorption at low pressure since the dynamic molecular diameter of CO₂ is 2.09 Å [36]. The key role of micropores for CO₂ adsorption at pressure lower than 1 bar has been reported in the literature [69]. CS-800 has the highest micropore volume amongst all CS prepared in this study (Table 1), it is then sensible to conclude that such a greater amount of micropores should be responsible for the enhance CO₂ capture performance of CS-800. Nonetheless, an appreciable start of plateau in the isotherms at pressure higher than 2 bar (Fig. 6a) implies that the CS cannot adsorb much more CO₂ at higher pressure confirming the lack of mesopores and an overall limited surface area. Because of its better CO₂ capture performance at low pressure CS-800 was selected for further characterizations under flue-gas-like conditions.

A typical coal-fired power plant emits flue gas made of approximately 15% CO₂ and 75% N₂, with balance of O₂, H₂O, sulfur oxides (SO_x), and nitrogen oxides (NO_x) [70].

Therefore, CO₂ sorbents for flue gas scrubbing should exhibit high selectivity for CO₂ over N₂ to ensure high CO₂ capture capacity even in the presence of nitrogen. Fig. 6c shows the CO₂ and N₂ uptake of CS-800 at 0 °C and 25 °C. As expected for physisorbents, the sorption capacity for both gasses are higher at lower temperature. The CO₂ capture selectivity values for CS-800 were determined based on the quantity of CO₂ and N₂ adsorbed at their relevant partial pressures (0.15 bar and 0.85 bar, respectively) as 23 and 30 at 0 °C and 25 °C, respectively. These selectivity values are comparable to those of other CS (Table S1), but in this case the CS were made without using any catalyst or activator. In addition, the variation of the CO₂/N₂ selectivities with pressures up to 10 bar is also presented in Fig. 6d. As can be observed, the selectivity decreases at higher pressure up to 7 bar.

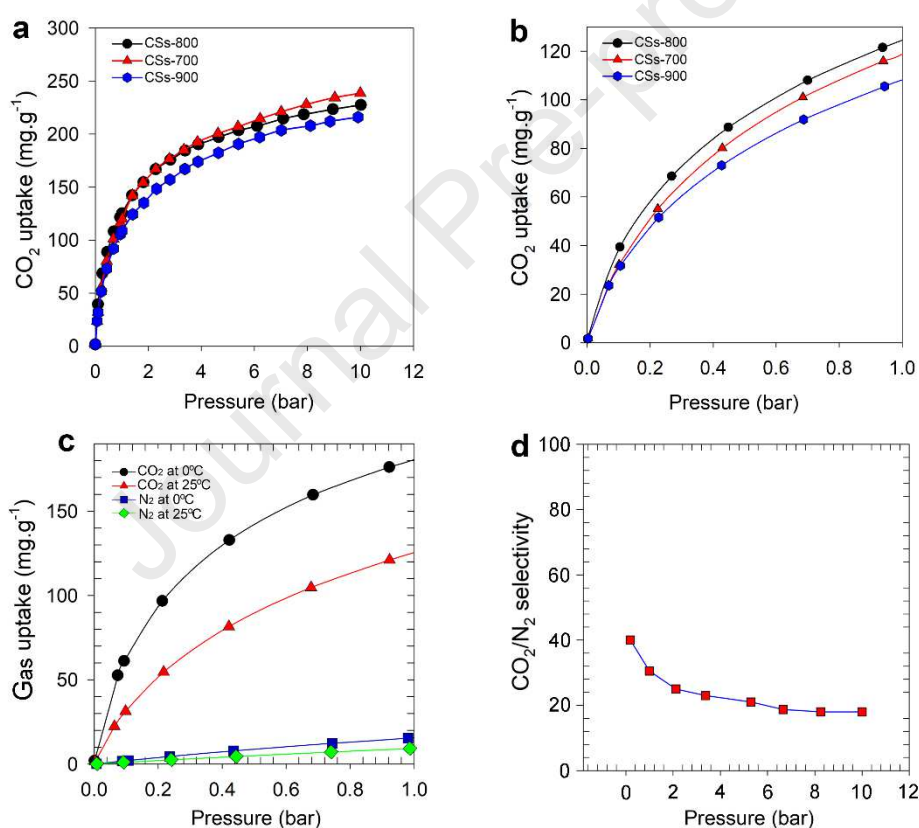


Fig. 6. CO₂ uptakes at 25 °C for the as prepared CS at pressures up to 10 bar (a) and 1 bar (b). CO₂ and N₂ uptakes at 0 °C to 25 °C, up to 1 bar for CS-800 (c). Isotherms for CO₂/N₂ selectivity of CS-800 at 25 °C and different pressures (d).

Although the surface area of the CS-800 is not very high, the main factors affecting CO₂ capture performance at ambient conditions are micropore volume and pore size,

properties for which the synthesized CS were tailored and perform excellently at low pressure compared to many other materials reported in the literature. It is worth to provide a few more comparisons of low-pressure performance between CS-800 and other carbon capture materials. Table 3 lists the capture performance of some benchmarks and some recently reported adsorbents. Notably, none of the CS prepared by CVD method (Table 2) are listed in Table 3 since they are non-porous or mesoporous, thus not suitable for CO₂ capture in ambient conditions. The CO₂ uptake of CS-800 in single component CO₂ at 0.15 bar and 25 °C is 1.1 mmol.g⁻¹, which is higher than the value reported for well-known benchmark materials such as BPL activated carbon and ZIF-8. In addition, typical CO₂ uptakes for some CS including hollow spheres (Table S1, Entry 6) are reported in Table S1. At 1 bar and 25 °C, CS-800 exhibits a relatively high CO₂ uptake of 2.85 mmol.g⁻¹, lower than KOH-activated CS but still significant since CS-800 are made without using any activator.

Another important CO₂ capture parameter is the isosteric heat of adsorption (Q_{st}), a measure of the heat released upon adsorption of CO₂. This heat impacts directly on the temperature of the sorption bed during the separation process.[71] The overall gas separation yield is strongly affected by local adsorption equilibria and kinetics which are function of the temperature of the bed. Here, the isosteric heat of adsorption of CS-800 was calculated using CO₂ adsorption isotherms measured at 25 °C, 35 °C, and 45 °C, and considering the nature of physical adsorption, the CO₂ uptake decreased with increasing temperature [72].

Table 3. Comparison of CO₂ capture capacity of some benchmarks and recently reported sorbents at 0.15 bar in single component CO₂.

Sorbent type	Temperature (°C)	Uptake (mmol/g)
BPL activated carbon ^a	25	0.8 [73]
ZIF-8 ^a	25	0.1 [73]
Zeolite-13X ^a	25	2.6 [73]
UiO-66 [F4_UiO-66(Ce)]	25	0.4 [74]
Holey graphene frameworks	25	0.5 [71]
KOH activated carbon ^b	25	0.8 [75]
Steam activated carbon ^c	25	0.5 [76]
rht-type MOF	0	2.6 [77]
Organic polyimides	0	1.2 [78]
CS-800	25	1.1 ^d

CS-800	0	1.8 ^d
--------	---	------------------

^aCommon benchmarks. ^bDerived from waste wool. ^cPrepared from melamine-modified phenol-formaldehyde resin. ^dThis work.

The resulting Q_{st} values were between 27.5–29.3 kJ mol⁻¹ for CO₂ uptakes between 0.7 and 3.4 mmol g⁻¹ (Fig. S11). As expected, the Q_{st} values were in the range of ordinary physisorption (<40 kJ mol⁻¹). In addition to selectivity and heat of adsorption, more realistic conditions should be considered for industrial applications. For example, cyclability and stability over multiple runs are critical factors in carbon capture applications. The cyclability of CS-800 was tested over 11 adsorption-desorption cycles with no appreciable deterioration of CO₂ capture capacity, ca. 1.89 mmol g⁻¹ (8.4 wt.%) working capacity (Fig. 7a). However, adsorption capacity decreases at 40 °C compared to 25 °C which is expected for physisorbents. The carbon spheres showed fast adsorption kinetics reaching saturation in less than 10 min, while complete regeneration required a longer time, 15 min at 40 °C in argon flow. Materials with ultramicroporosity like CS-800 are characterized by desorption hysteresis due to entrapment of CO₂ molecules in pores of the size of a few CO₂ diameters causing desorption delays.

Combustion flue gases contain moisture, and CO₂ capture in humid streams is known to be affected by the presence of water. For this reason, the CO₂ capture performance of the carbon spheres was tested using CO₂ bubbled through deionized water to produce a stream of wet CO₂. A sample of CS-800 was exposed to wet CO₂ while monitoring its weight with a TGA [79], the results are shown in Fig. 7b. The wet CO₂ experiment consisted of three steps performed with different gases at a fixed temperature of 40 °C. In the first step, a sample of CS-800 (previously treated in dry Ar at 140 °C to remove any adsorbed species) was exposed to a 100 ml min⁻¹ flow of wet Ar (argon bubbled through deionized water) leading to an increase of weight of almost 1.5 wt.% as a result of the partial hydration of CS-800. In the second step, the gas flow was switched to 95 ml min⁻¹ wet CO₂, resulting in a jump of weight of ca. 7 wt.%. This rapid uptake was associated to CO₂ adsorption since the sorbent was already fully saturated with water. Although a CO₂ uptake of ~6.0 wt.% (1.3 mmol g⁻¹) in humid conditions is slightly lower than that recorded in dry gas stream 8.3 wt.% (1.8 mmol g⁻¹), sorption kinetics remained fast highlight the good performance of CS-800. In the third and final step, the sorbent was exposed again to dry Ar for desorption, both water and CO₂ were rapidly released with no need of heating. As expected from high hydrophobicity and microporosity of the carbon

spheres, CS-800 did not host water molecules to a large extent maintaining the ability to adsorb significant amount of CO₂ even in wet conditions. This is an advantage over some zeolites and MOFs that underperform in humid conditions.

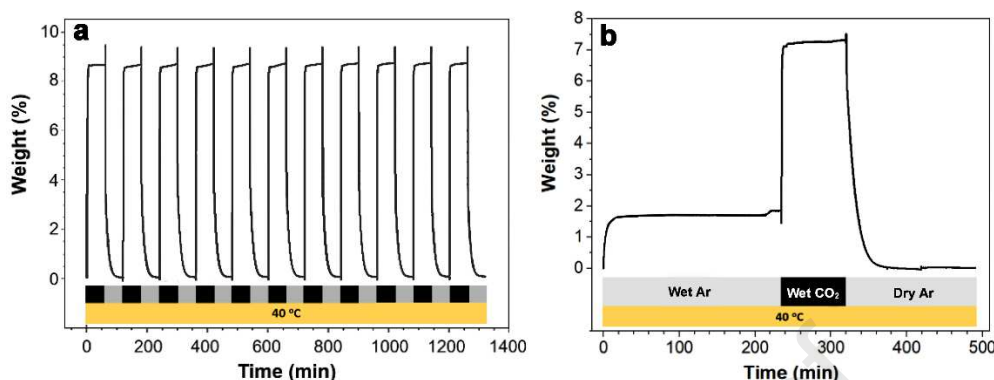


Fig. 7. CS-800 adsorption-desorption studies at 40 °C. Cyclability test of adsorption in single component CO₂ (black sections) and desorption in dry Ar (grey sections) (a). CO₂ capture performance in wet gas streams, wet Ar and wet CO₂, followed by desorption in dry Ar (b).

Nowadays, the most common process of production of pyromellitic acid is based on the oxidation of durene, a product of oil refinery, but the green and sustainable production of pyromellitic acid from pinacol and diethyl maleate has been reported in the literature [80]. Pyromellitic acid is a key precursor in the large-scale production of polyimide, and from an industry point of view, the cost of feedstocks is very important. In this regard, Table S2 lists the market price of pyromellitic acid from different suppliers. Pyromellitic acid from both retail and wholesale sources are reasonably cheap, making the process of microporous CS production presented in this manuscript of potential interest for large-scale production. As a yield of ~30% can be estimated from details mentioned in experimental section, for example, the cost of feedstock for 1 ton of CS would be around \$6000 (\$1/kg pyromellitic acid; 5.8 kg of pyromellitic acid per 1 kg of CS). This cost does not include capital and operational costs; however, it is very important to highlight that there would be no additional cost for solvents or catalysts, neither for separation or purification processes. There are also some prospects which can likely improve the yield of final CSs such as applying a high-performance filter in the exhaust part and using a longer tube in order to provide more surface for CSs deposition in Zone 2. More research in this regard is under progress.

4. Conclusions

We report here the successful green one-step CVD preparation method of ultramicroporous carbon spheres using a safe solid feedstock. This novel CVD method enabled the self-assembly of spheres from cheap readily available in the market pyromellitic acid with no need of either a catalyst or an activator. Pyromellitic dianhydride can also be used in place of pyromellitic acid to make the same CS, however the anhydride is not environmentally friendly while the acid is. In accordance with green chemistry principles, pyromellitic acid should be used for this process. The as-prepared CS possesses a large number of narrow pores smaller than 1 nm making them good CO₂ post-combustion capture materials. Ultramicroporous CS can be made at 700 °C, 800 °C, and 900 °C. The CO₂ uptake at 1 bar in single component gas stream was determined as follows: CS-800 (2.85 mmol g⁻¹) > CS-700 (2.65 mmol g⁻¹) > CS-900 (2.45 mmol g⁻¹). In all cases, the CO₂ uptake efficiency is governed by narrow micropores mostly less than 10 Å. However, the CO₂ capture performance of CS-800 was found high particularly for uptakes at lower pressures. In addition, the CO₂ selectivity over N₂ at 25 °C was determined as 30:1 which was higher or comparable to other reported activated carbon spheres for post-combustion capture, making this CS suitable for CO₂ separation from flue gases. The present method for the synthesis of CS provides several green chemistry benefits including (i) alkali-free and (ii) catalyst-free pyrolysis, (iii) the use of a cheap and safe feedstock readily available in the market, and (iv) a rapid and safe procedure with (v) no need of solvents for purification. In a wider perspective, the present method is a valid alternative to other CVD methods that rely on hazardous gas and liquid feedstocks for large scale carbon sphere production. Due to the growing interest in the use of carbon spheres in batteries and supercapacitors, our CS might also contribute to the development of renewable energy storage technologies.

Acknowledgements

S. K. wishes to acknowledge funding from the European Union's Horizon 2020 research and innovation programme under the Marie Skłodowska-Curie grant agreement No 663830. S. K. and E. A. also wish to thank the Engineering and Physical Sciences Research Council-Impact Acceleration Account (EPSRC-IAA) for providing funding to project code RIF67. Financial support was also provided by the Reduce Industrial Carbon Emissions (RICE) and Flexible Integrated Energy Systems (FLEXIS) research operations part funded by the EU's European Regional Development Fund through the Welsh

Government. The authors would also like to acknowledge the assistance provided by the Swansea University AIM Facility, which was funded in part by the EPSRC (EP/M028267/1), the European Regional Development Fund through the Welsh Government (80708) and the Sêr Solar project via the Welsh Government. Dr Louise Hamdy and Dr James McGettrick are also thanked for their help with the TGA and XPS analyses.

References

- [1] J. Liu, N.P. Wickramaratne, S.Z. Qiao, M. Jaroniec, Molecular-based design and emerging applications of nanoporous carbon spheres, *Nature Materials* 14 (2015) 763.
- [2] X. Kan, X. Chen, W. Chen, J. Mi, J.-Y. Zhang, F. Liu, A. Zheng, K. Huang, L. Shen, C. Au, L. Jiang, Nitrogen-Decorated, Ordered Mesoporous Carbon Spheres as High-Efficient Catalysts for Selective Capture and Oxidation of H₂S, *ACS Sustainable Chemistry & Engineering* 7(8) (2019) 7609-7618.
- [3] J. Pang, W. Zhang, H. Zhang, J. Zhang, H. Zhang, G. Cao, M. Han, Y. Yang, Sustainable nitrogen-containing hierarchical porous carbon spheres derived from sodium lignosulfonate for high-performance supercapacitors, *Carbon* 132 (2018) 280-293.
- [4] P. Zhang, Z.-A. Qiao, S. Dai, Recent advances in carbon nanospheres: synthetic routes and applications, *Chemical Communications* 51(45) (2015) 9246-9256.
- [5] W. Kukulka, K. Wenelska, M. Baca, X. Chen, E. Mijowska, From Hollow to Solid Carbon Spheres: Time-Dependent Facile Synthesis, *Nanomaterials* 8(10) (2018).
- [6] P. Liu, W. Cai, J. Wei, Z. Cai, M. Zhu, B. Han, Z. Yang, J. Chen, M. Jaroniec, Ultrafast preparation of saccharide-derived carbon microspheres with excellent dispersibility via ammonium persulfate-assisted hydrothermal carbonization, *Journal of Materials Chemistry A* 7(32) (2019) 18840-18845.
- [7] H. Kristianto, C.D. Putra, A.A. Arie, M. Halim, J.K. Lee, Synthesis and Characterization of Carbon Nanospheres Using Cooking Palm Oil as Natural Precursors onto Activated Carbon Support, *Procedia Chemistry* 16 (2015) 328-333.
- [8] G.G. Karthikeyan, G. Boopathi, A. Pandurangan, Facile Synthesis of Mesoporous Carbon Spheres Using 3D Cubic Fe-KIT-6 by CVD Technique for the Application of Active Electrode Materials in Supercapacitors, *ACS Omega* 3(12) (2018) 16658-16671.
- [9] A.C. Dassanayake, N.P. Wickramaratne, M.A. Hossain, V.S. Perera, J. Jeskey, S.D. Huang, H. Shen, M. Jaroniec, Prussian blue-assisted one-pot synthesis of nitrogen-doped mesoporous graphitic carbon spheres for supercapacitors, *Journal of Materials Chemistry A* (2019).
- [10] S. Li, A. Pasc, V. Fierro, A. Celzard, Hollow carbon spheres, synthesis and applications – a review, *Journal of Materials Chemistry A* 4(33) (2016) 12686-12713.
- [11] J. Liu, T. Yang, D.-W. Wang, G.Q. Lu, D. Zhao, S.Z. Qiao, A facile soft-template synthesis of mesoporous polymeric and carbonaceous nanospheres, *Nature Communications* 4(1) (2013) 2798.
- [12] X. Liu, P. Song, J. Hou, B. Wang, F. Xu, X. Zhang, Revealing the Dynamic Formation Process and Mechanism of Hollow Carbon Spheres: From Bowl to Sphere, *ACS Sustainable Chemistry & Engineering* 6(2) (2018) 2797-2805.
- [13] J. Kang, O.L. Li, N. Saito, Synthesis of structure-controlled carbon nano spheres by solution plasma process, *Carbon* 60 (2013) 292-298.

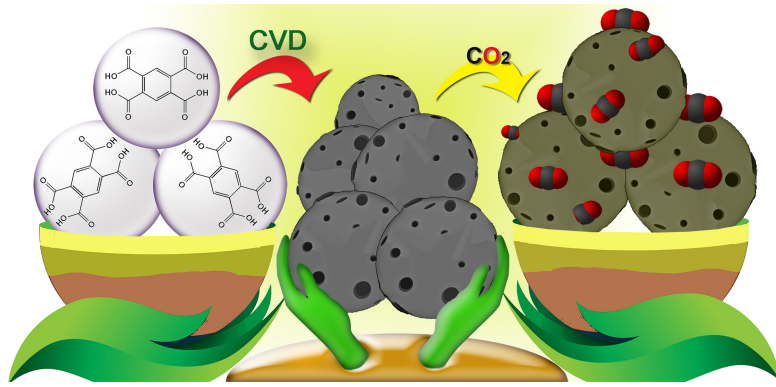
- [14] G. Wang, R. Wang, L. Liu, H. Zhang, J. Du, Y. Zhang, M. Liu, K. Liang, A. Chen, Synthesis of hollow mesoporous carbon spheres via Friedel-Crafts reaction strategy for supercapacitor, *Materials Letters* 197 (2017) 71-74.
- [15] X. Zhao, W. Li, F. Kong, H. Chen, Z. Wang, S. Liu, C. Jin, Carbon spheres derived from biomass residue via ultrasonic spray pyrolysis for supercapacitors, *Materials Chemistry and Physics* 219 (2018) 461-467.
- [16] X. Li, S. Bai, Z. Zhu, J. Sun, X. Jin, X. Wu, J. Liu, Hollow Carbon Spheres with Abundant Micropores for Enhanced CO₂ Adsorption, *Langmuir* 33(5) (2017) 1248-1255.
- [17] Y. Li, S. Wang, B. Wang, Y. Wang, J. Wei, Sustainable Biomass Glucose-Derived Porous Carbon Spheres with High Nitrogen Doping: As a Promising Adsorbent for CO₂/CH₄/N₂ Adsorptive Separation, *Nanomaterials* 10(1) (2020) 174.
- [18] Z. Bi, Q. Kong, Y. Cao, G. Sun, F. Su, X. Wei, X. Li, A. Ahmad, L. Xie, C.-M. Chen, Biomass-derived porous carbon materials with different dimensions for supercapacitor electrodes: a review, *Journal of Materials Chemistry A* 7(27) (2019) 16028-16045.
- [19] A. Rashidi, M.K. Abbasabadi, S. Khodabakhshi, Allylamide-grafted multiwall carbon nanotubes as a new type of nanoadsorbent for the H₂S removal from gas stream, *Journal of Natural Gas Science and Engineering* 36 (2016) 13-19.
- [20] A.W. Orbaek, A.R. Barron, Towards a 'catalyst activity map' regarding the nucleation and growth of single walled carbon nanotubes, *Journal of Experimental Nanoscience* 10(1) (2015) 66-76.
- [21] Y. Zhang, L. Zhang, C. Zhou, Review of Chemical Vapor Deposition of Graphene and Related Applications, *Accounts of Chemical Research* 46(10) (2013) 2329-2339.
- [22] J. Prasek, J. Drbohlavova, J. Chomoucka, J. Hubalek, O. Jasek, V. Adam, R. Kizek, Methods for carbon nanotubes synthesis—review, *Journal of Materials Chemistry* 21(40) (2011) 15872-15884.
- [23] D. Tong, Q. Zhang, Y. Zheng, K. Caldeira, C. Shearer, C. Hong, Y. Qin, S.J. Davis, Committed emissions from existing energy infrastructure jeopardize 1.5 °C climate target, *Nature* 572(7769) (2019) 373-377.
- [24] R. Yousefi, T.J. Struble, J.L. Payne, M. Vishe, N.D. Schley, J.N. Johnston, Catalytic, Enantioselective Synthesis of Cyclic Carbamates from Dialkyl Amines by CO₂-Capture: Discovery, Development, and Mechanism, *Journal of the American Chemical Society* 141(1) (2019) 618-625.
- [25] M. Bui, C.S. Adjiman, A. Bardow, E.J. Anthony, A. Boston, S. Brown, P.S. Fennell, S. Fuss, A. Galindo, L.A. Hackett, J.P. Hallett, H.J. Herzog, G. Jackson, J. Kemper, S. Krevor, G.C. Maitland, M. Matuszewski, I.S. Metcalfe, C. Petit, G. Puxty, J. Reimer, D.M. Reiner, E.S. Rubin, S.A. Scott, N. Shah, B. Smit, J.P.M. Trusler, P. Webley, J. Wilcox, N. Mac Dowell, Carbon capture and storage (CCS): the way forward, *Energy & Environmental Science* 11(5) (2018) 1062-1176.
- [26] E.P. Dillon, C.A. Crouse, A.R. Barron, Synthesis, Characterization, and Carbon Dioxide Adsorption of Covalently Attached Polyethyleneimine-Functionalized Single-Wall Carbon Nanotubes, *ACS Nano* 2(1) (2008) 156-164.
- [27] E. Andreoli, E.P. Dillon, L. Cullum, L.B. Alemany, A.R. Barron, Cross-Linking Amine-Rich Compounds into High Performing Selective CO₂ Absorbents, *Scientific Reports* 4(1) (2014) 7304.
- [28] Z. Zhang, Z.P. Cano, D. Luo, H. Dou, A. Yu, Z. Chen, Rational design of tailored porous carbon-based materials for CO₂ capture, *Journal of Materials Chemistry A* 7(37) (2019) 20985-21003.
- [29] S. Ghosh, A.R. Barron, Optimizing Carbon Dioxide Uptake and Carbon Dioxide-Methane Selectivity of Oxygen-Doped Porous Carbon Prepared from Oxygen Containing Polymer Precursors, *ChemistrySelect* 2(36) (2017) 11959-11968.

- [30] T. Du, X. Fang, L. Liu, J. Shang, B. Zhang, Y. Wei, H. Gong, S. Rahman, E.F. May, P.A. Webley, G. Li, An optimal trapdoor zeolite for exclusive admission of CO₂ at industrial carbon capture operating temperatures, *Chemical Communications* 54(25) (2018) 3134-3137.
- [31] M. Jahandar Lashaki, S. Khiavi, A. Sayari, Stability of amine-functionalized CO₂ adsorbents: a multifaceted puzzle, *Chemical Society Reviews* 48(12) (2019) 3320-3405.
- [32] M. Jahandar Lashaki, H. Ziaei-Azad, A. Sayari, Insights into the Hydrothermal Stability of Triamine-Functionalized SBA-15 Silica for CO₂ Adsorption, *ChemSusChem* 10(20) (2017) 4037-4045.
- [33] G.A. Mutch, S. Shulda, A.J. McCue, M.J. Menart, C.V. Ciobanu, C. Ngo, J.A. Anderson, R.M. Richards, D. Vega-Maza, Carbon Capture by Metal Oxides: Unleashing the Potential of the (111) Facet, *Journal of the American Chemical Society* 140(13) (2018) 4736-4742.
- [34] M. Ding, R.W. Flaig, H.-L. Jiang, O.M. Yaghi, Carbon capture and conversion using metal-organic frameworks and MOF-based materials, *Chemical Society Reviews* 48(10) (2019) 2783-2828.
- [35] J. Liu, P.K. Thallapally, B.P. McGrail, D.R. Brown, J. Liu, Progress in adsorption-based CO₂ capture by metal-organic frameworks, *Chemical Society Reviews* 41(6) (2012) 2308-2322.
- [36] N. Sun, C. Sun, J. Liu, H. Liu, C.E. Snape, K. Li, W. Wei, Y. Sun, Surface-modified spherical activated carbon materials for pre-combustion carbon dioxide capture, *RSC Advances* 5(42) (2015) 33681-33690.
- [37] J. Ludwinowicz, M. Jaroniec, Potassium salt-assisted synthesis of highly microporous carbon spheres for CO₂ adsorption, *Carbon* 82 (2015) 297-303.
- [38] P. Mohanty, L.D. Kull, K. Landskron, Porous covalent electron-rich organonitridic frameworks as highly selective sorbents for methane and carbon dioxide, *Nature Communications* 2(1) (2011) 401.
- [39] J. Marszewska, M. Jaroniec, Tailoring porosity in carbon spheres for fast carbon dioxide adsorption, *Journal of Colloid and Interface Science* 487 (2017) 162-174.
- [40] A. Chen, S. Li, Y. Yu, L. Liu, Y. Li, Y. Wang, K. Xia, Self-catalyzed strategy to form hollow carbon nanospheres for CO₂ capture, *Materials Letters* 185 (2016) 63-66.
- [41] X. Ren, H. Li, J. Chen, L. Wei, A. Modak, H. Yang, Q. Yang, N-doped porous carbons with exceptionally high CO₂ selectivity for CO₂ capture, *Carbon* 114 (2017) 473-481.
- [42] Z. Zhang, D. Luo, G. Lui, G. Li, G. Jiang, Z.P. Cano, Y.-P. Deng, X. Du, S. Yin, Y. Chen, M. Zhang, Z. Yan, Z. Chen, In-situ ion-activated carbon nanospheres with tunable ultramicroporosity for superior CO₂ capture, *Carbon* 143 (2019) 531-541.
- [43] E. Fernandez-Bartolome, J. Santos, A. Gamonal, S. Khodabakhshi, L.J. McCormick, S.J. Teat, E.C. Sañudo, J.S. Costa, N. Martín, A Three-Dimensional Dynamic Supramolecular “Sticky Fingers” Organic Framework, *Angewandte Chemie International Edition* 58(8) (2019) 2310-2315.
- [44] E. Andreoli, A.R. Barron, Effect of spray-drying and cryo-milling on the CO₂ absorption performance of C₆₀ cross-linked polyethyleneimine, *Journal of Materials Chemistry A* 3(8) (2015) 4323-4329.
- [45] E. Andreoli, E.P. Dillon, L. Cullum, L.B. Alemany, A.R. Barron, Cross-Linking Amine-Rich Compounds into High Performing Selective CO₂ Absorbents, *Scientific Reports* 4 (2014) 7304.
- [46] A. Koutsianos, A.R. Barron, E. Andreoli, CO₂ Capture Partner Molecules in Highly Loaded PEI Sorbents, *The Journal of Physical Chemistry C* 121(39) (2017) 21772-21781.

- [47] A.B. Elmas Kimyonok, M. Ulutürk, Determination of the Thermal Decomposition Products of Terephthalic Acid by Using Curie-Point Pyrolyzer, *Journal of Energetic Materials* 34(2) (2016) 113-122.
- [48] T. Kosaka, Y. Sakai, Process for preparing pyromellitic dianhydride, Google Patents, 1987.
- [49] W. Wagner, F. Muller, H.-J. Eberle, F. Grundei, Process for preparing pyromellitic dianhydride, Google Patents, 1995.
- [50] P. Kumar, R. Meena, R. Paulraj, A. Chanchal, A.K. Verma, H.B. Bohidar, Fluorescence behavior of non-functionalized carbon nanoparticles and their in vitro applications in imaging and cytotoxic analysis of cancer cells, *Colloids and Surfaces B: Biointerfaces* 91 (2012) 34-40.
- [51] V.N. Tsaneva, W. Kwapinski, X. Teng, B.A. Glowacki, Assessment of the structural evolution of carbons from microwave plasma natural gas reforming and biomass pyrolysis using Raman spectroscopy, *Carbon* 80 (2014) 617-628.
- [52] R.F. Egerton, Mechanisms of radiation damage in beam-sensitive specimens, for TEM accelerating voltages between 10 and 300 kV, *Microscopy Research and Technique* 75(11) (2012) 1550-1556.
- [53] S.-M. Hong, E. Jang, A.D. Dysart, V.G. Pol, K.B. Lee, CO₂ Capture in the Sustainable Wheat-Derived Activated Microporous Carbon Compartments, *Scientific Reports* 6(1) (2016) 34590.
- [54] W. Yang, S. Mao, J. Yang, T. Shang, H. Song, J. Mabon, W. Swiech, J.R. Vance, Z. Yue, S.J. Dillon, H. Xu, B. Xu, Large-deformation and high-strength amorphous porous carbon nanospheres, *Scientific Reports* 6 (2016) 24187.
- [55] J. Díaz, G. Paolicelli, S. Ferrer, F. Comin, Separation of the sp^3 and sp^2 components in the C1s photoemission spectra of amorphous carbon films, *Phys. Rev. B: Condens. Matter* 54(11) (1996) 8064-8069.
- [56] A. Ganguly, S. Sharma, P. Papakonstantinou, J. Hamilton, Probing the Thermal Deoxygenation of Graphene Oxide Using High-Resolution In Situ X-ray-Based Spectroscopies, *The Journal of Physical Chemistry C* 115(34) (2011) 17009-17019.
- [57] G. Kupgan, T.P. Liyana-Arachchi, C.M. Colina, NLDFT Pore Size Distribution in Amorphous Microporous Materials, *Langmuir* 33(42) (2017) 11138-11145.
- [58] G.L. Aranovich, M.D. Donohue, Adsorption isotherms for microporous adsorbents, *Carbon* 33(10) (1995) 1369-1375.
- [59] A. Rehman, S.-J. Park, From chitosan to urea-modified carbons: Tailoring the ultra-microporosity for enhanced CO₂ adsorption, *Carbon* 159 (2020) 625-637.
- [60] M. Molina-Sabio, M.T. Gonzalez, F. Rodriguez-Reinoso, A. Sepúlveda-Escribano, Effect of steam and carbon dioxide activation in the micropore size distribution of activated carbon, *Carbon* 34(4) (1996) 505-509.
- [61] J.A. Carrasco, H. Prima-Garcia, J. Romero, J. Hernández-Saz, S.I. Molina, G. Abellán, E. Coronado, CVD synthesis of carbon spheres using NiFe-LDHs as catalytic precursors: structural, electrochemical and magnetoresistive properties, *Journal of Materials Chemistry C* 4(3) (2016) 440-448.
- [62] J.-Y. Miao, D.W. Hwang, K.V. Narasimhulu, P.-I. Lin, Y.-T. Chen, S.-H. Lin, L.-P. Hwang, Synthesis and properties of carbon nanospheres grown by CVD using Kaolin supported transition metal catalysts, *Carbon* 42(4) (2004) 813-822.
- [63] X. Chen, K. Kierzek, K. Cendrowski, I. Pelech, X. Zhao, J. Feng, R.J. Kalenczuk, T. Tang, E. Mijowska, CVD generated mesoporous hollow carbon spheres as supercapacitors, *Colloids and Surfaces A: Physicochemical and Engineering Aspects* 396 (2012) 246-250.

- [64] K.P. Tripathi, S. Durbach, J.N. Coville, CVD Synthesis of Solid, Hollow, and Nitrogen-Doped Hollow Carbon Spheres from Polypropylene Waste Materials, *Applied Sciences* 9(12) (2019).
- [65] Y.Z. Jin, C. Gao, W.K. Hsu, Y. Zhu, A. Huczko, M. Bystrzejewski, M. Roe, C.Y. Lee, S. Acquah, H. Kroto, D.R.M. Walton, Large-scale synthesis and characterization of carbon spheres prepared by direct pyrolysis of hydrocarbons, *Carbon* 43(9) (2005) 1944-1953.
- [66] A.L.C. Lima, J.W. Farrington, C.M. Reddy, Combustion-Derived Polycyclic Aromatic Hydrocarbons in the Environment—A Review, *Environmental Forensics* 6(2) (2005) 109-131.
- [67] S. Khodabakhshi, P.F. Fulvio, E. Andreoli, Carbon black reborn: Structure and chemistry for renewable energy harnessing, *Carbon* 162 (2020) 604-649.
- [68] S.L.Y. Tang, R.L. Smith, M. Poliakoff, Principles of green chemistry: PRODUCTIVELY, *Green Chemistry* 7(11) (2005) 761-762.
- [69] V. Presser, J. McDonough, S.-H. Yeon, Y. Gogotsi, Effect of pore size on carbon dioxide sorption by carbide derived carbon, *Energy & Environmental Science* 4(8) (2011) 3059-3066.
- [70] A. Li, J. Wang, B. Bao, High-efficiency CO₂ capture and separation based on hydrate technology: A review, *Greenhouse Gases: Science and Technology* 9(2) (2019) 175-193.
- [71] S. Chowdhury, R. Balasubramanian, Holey graphene frameworks for highly selective post-combustion carbon capture, *Scientific Reports* 6 (2016) 21537.
- [72] J. Liu, X. Liu, Y. Sun, C. Sun, H. Liu, L.A. Stevens, K. Li, C.E. Snape, High Density and Super Ultra-Microporous-Activated Carbon Macrospheres with High Volumetric Capacity for CO₂ Capture, *Advanced Sustainable Systems* 2(2) (2018) 1700115.
- [73] J. McEwen, J.-D. Hayman, A. Ozgur Yazaydin, A comparative study of CO₂, CH₄ and N₂ adsorption in ZIF-8, Zeolite-13X and BPL activated carbon, *Chemical Physics* 412 (2013) 72-76.
- [74] R. D'Amato, A. Donnadio, M. Carta, C. Sangregorio, D. Tiana, R. Vivani, M. Taddei, F. Costantino, Water-Based Synthesis and Enhanced CO₂ Capture Performance of Perfluorinated Cerium-Based Metal–Organic Frameworks with UiO-66 and MIL-140 Topology, *ACS Sustainable Chemistry & Engineering* 7(1) (2019) 394-402.
- [75] Y. Li, R. Xu, B. Wang, J. Wei, L. Wang, M. Shen, J. Yang, Enhanced N-doped Porous Carbon Derived from KOH-Activated Waste Wool: A Promising Material for Selective Adsorption of CO₂/CH₄ and CH₄/N₂, *Nanomaterials* 9(2) (2019).
- [76] R.-L. Tseng, F.-C. Wu, R.-S. Juang, Adsorption of CO₂ at atmospheric pressure on activated carbons prepared from melamine-modified phenol–formaldehyde resins, *Separation and Purification Technology* 140 (2015) 53-60.
- [77] B. Li, Z. Zhang, Y. Li, K. Yao, Y. Zhu, Z. Deng, F. Yang, X. Zhou, G. Li, H. Wu, N. Nijem, Y.J. Chabal, Z. Lai, Y. Han, Z. Shi, S. Feng, J. Li, Enhanced Binding Affinity, Remarkable Selectivity, and High Capacity of CO₂ by Dual Functionalization of a rht-Type Metal–Organic Framework, *Angewandte Chemie International Edition* 51(6) (2012) 1412-1415.
- [78] C. Xu, N. Hedin, Synthesis of microporous organic polymers with high CO₂-over-N₂ selectivity and CO₂ adsorption, *Journal of Materials Chemistry A* 1(10) (2013) 3406-3414.
- [79] L.B. Hamdy, R.J. Wakeham, M. Taddei, A.R. Barron, E. Andreoli, Epoxy Cross-Linked Polyamine CO₂ Sorbents Enhanced via Hydrophobic Functionalization, *Chemistry of Materials* 31(13) (2019) 4673-4684.
- [80] Y. Hu, N. Li, G. Li, A. Wang, Y. Cong, X. Wang, T. Zhang, Sustainable production of pyromellitic acid with pinacol and diethyl maleate, *Green Chemistry* 19(7) (2017) 1663-1667.

Journal Pre-proof



Journal Pre-proof

Highlights

- A green, rapid, and scalable method to prepare microporous carbon spheres was developed.
- A safe and solid feedstock was used for CVD synthesis of carbon sphere.
- The presented CVD method was template and catalyst-free.
- Carbon spheres with high abundance of ultramicropores were obtained without any activating agents.
- Self-activated carbon spheres were tested for CO₂ capture and showed good capacity for low pressure CO₂ capture.

Declaration of interests

The authors declare that they have no known competing financial interests or personal relationships that could have appeared to influence the work reported in this paper.

The authors declare the following financial interests/personal relationships which may be considered as potential competing interests:

Journal Pre-proof